Development 125, 3123-3132 (1998)
Printed in Great Britain © The Company of Biologists Limited 1998
DEV2276

Evidence that preaxial polydactyly in the *Doublefoot* mutant is due to ectopic Indian Hedgehog signaling

Yingzi Yang[1], Pascale Guillot[2], Yvonne Boyd[2], Mary F. Lyon[2] and Andrew P. McMahon[1,*]

[1]Department of Molecular and Cellular Biology, The Biolabs, Harvard University, 16 Divinity Ave., Cambridge, MA 02138, USA
[2]Mammalian Genetics Unit, Medical Research Council, Harwell, Didcot, Oxon OX11 0RD, UK
*Author for correspondence (amcmahon@biosun.harvard.edu)

Accepted 10 June; published on WWW 21 July 1998

SUMMARY

Patterning of the vertebrate limb along the anterior-posterior axis is controlled by the zone of polarizing activity (ZPA) located at the posterior limb margin. One of the vertebrate *Hh* family members, *Shh*, has been shown to be able to mediate the function of the ZPA. Several naturally occurring mouse mutations with the phenotype of preaxial polydactyly exhibit ectopic *Shh* expression at the anterior limb margin. In this study, we report the molecular characterization of a spontaneous mouse mutation, *Doublefoot* (*Dbf*). *Dbf* is a dominant mutation which maps to chromosome 1. Heterozygous and homozygous embryos display a severe polydactyly with 6 to 8 digits on each limb. We show here that *Shh* is expressed normally in *Dbf* mutants. In contrast, a second *Hh* family member, *Indian hedgehog* (*Ihh*) which maps close to *Dbf*, is ectopically expressed in the distal limb bud. Ectopic *Ihh* expression in the distal and anterior limb bud results in the ectopic activation of several genes associated with anterior-posterior and proximal-distal patterning (*Fgf4*, *Hoxd13*, *Bmp2*). In addition, specific components in the *Hedgehog* pathway are either ectopically activated (*Ptc*, *Ptc-2*, *Gli1*) or repressed (*Gli2*). We propose that misexpression of *Ihh*, and not a novel Smoothened ligand as recently suggested (Hayes et al., 1998), is responsible for the *Dbf* phenotype. We consider that *Ihh* has a similar activity to *Shh* when expressed in the early *Shh*-responsive limb bud. To determine whether *Dbf* maps to the *Ihh* locus, which is also on chromosome 1, we performed an interspecific backcross. These results demonstrate that *Dbf* and *Ihh* are genetically separated by approximately 1.3 centimorgans, suggesting that *Dbf* mutation may cause an exceptionally long-range disruption of *Ihh* regulation. Although this leads to ectopic activation of *Ihh*, normal expression of *Ihh* in the cartilaginous elements is retained.

Key words: *Indian hedgehog*, Polydactyly, *Doublefoot* mutant, Mouse, Limb patterning

INTRODUCTION

The vertebrate limb serves as a model system for studying the control of pattern formation. Classic embryonic studies in the chick limb have revealed three signaling centers, namely the AER (Apical Ectodermal Ridge), ZPA (Zone of Polarizing Activity) and limb bud ectoderm, that control the growth and patterning along the proximal-distal (P-D), anterior-posterior (A-P) and dorsal-ventral (D-V) axes respectively. Insight into the nature of these patterning processes has been revealed through the identification of signaling molecules that appear to mediate the function of these signaling centers. Members of the *Fgf* (*Fibroblast Growth Factor*) family such as *Fgf2*, *Fgf4* and *Fgf8* (Niswander et al., 1993; Fallon, et al., 1994; Crossley and Martin, 1995) are capable of substituting for the function of the AER. *Sonic hedgehog* (*Shh*), a member of the vertebrate *Hedgehog* (*Hh*) family (Echelard et al., 1993), can mediate the function of the ZPA (Riddle et al., 1993; Laufer et al., 1994; Niswander et al., 1994; Lopez-Martinez et al., 1995; Yang et al., 1997). *Wnt7a*, a member of the vertebrate *Wnt* family, controls the determination of dorsal fate in the distal limb through the regulation of transcription factor *Lmx1b*, a vertebrate homologue of *Drosophila apterous* (Parr and McMahon, 1995; Riddle et al., 1995; Cygan et al., 1997). In addition, *En-1*, a homeobox transcription factor expressed specifically in the ventral ectoderm determines ventral cell fate by suppressing *Wnt7a* expression (Cygan et al., 1997; Loomis et al., 1998). Moreover, the chick and mouse studies demonstrate that molecules from the three signaling centers interact with each other to coordinately control limb development along the three axes (for review, see Johnson and Tabin, 1997).

A challenge in studying vertebrate limb development is to understand how these signaling molecules are integrated in their physiological context. The existence of several naturally occurring mouse mutants that affect limb development has provided an opportunity to further study the regulatory mechanisms underlying limb patterning. For instance, several naturally occurring mouse mutations with the phenotype of polydactyly have been shown to affect the A-P patterning of

the limb, especially the hindlimb. Their phenotypes have been characterized and the mutations genetically mapped. Among the polydactyly mutants, preaxial polydactyly with malformation of the radius or tibia represents a major group. Studies carried out in several research groups have shown that mouse mutations *luxate* (*lx*), *Strong's luxoid* (*lst*), *X-linked polydactyly* (*Xpl*), *Recombination induced mutant 4* (*Rim4*), *Hemimelic extra toes* (*Hx*) and *Extra toes* (*Xt*) (Chan et al., 1995; Buscher et al., 1997; Masuya et al., 1995, 1997) exhibit mirror image duplication of anterior digits. These defects are most likely caused by the anterior formation of an ectopic ZPA, since *Shh* and *Fgf4* are ectopically expressed at the anterior margin of these mutant limbs. Furthermore, tissue grafting experiments show that the anterior limb bud of the *lst* mutant has polarizing activity (Chan et al., 1995). However, the molecular mechanism of ectopic expression of *Shh* and *Fgf4* is poorly understood except for the case of *Xt*, which has been shown to be a loss-of-function mutation in the *Gli3* gene (Vortkamp et al., 1992; Hui and Joyner, 1993). *Ci* (*Cubitus interruptus*, the *Drosophila* homologue of *Gli3*) has been shown to inhibit the expression of *Hh* in the anterior compartment of *Drosophila* wing disc, consistent with a similar role for *Gli3* in vertebrate limb development (Dominguez et al., 1996). Studies of preaxial polydactyly mutants may eventually lead to the identification of the molecular pathway that serves to set up and restrict the endogenous ZPA to the posterior limb margin.

Apart from the mutations that occurred naturally, genetic manipulations in the mouse have revealed other candidates for ZPA regulation. *Alx4*, a paired-type homeodomain protein expressed in the anterior mesenchyme of the limb, also appears to restrict ZPA formation to the posterior limb margin by inhibiting the expression of *Shh* at the anterior limb margin (Qu et al., 1997). *Hoxb8*, a homeobox transcription factor, is a candidate determinant to position the polarizing activity at the posterior margin of the future limb bud. When ectopically expressed in the entire proximal forelimb bud, *Hoxb8* induces ectopic *Shh* expression at the anterior limb margin (Charite et al., 1994). These studies suggest that the restriction of *Shh* expression to the posterior margin may involve at least two mechanisms: the presence of transcriptional inhibitors and the absence of transcriptional activators of *Shh* expression at the anterior limb margin.

Two other *hedgehog* family members have been identified in the mouse, *Indian hedgehog* (*Ihh*) and *Desert hedgehog* (*Dhh*) (Echelard et al., 1993). Neither gene is expressed in the distal limb bud where patterning occurs, but *Ihh* is expressed in the condensed cartilage and is required for cartilage development (Vortkamp et al., 1996; B. St-Jacques, M. Hammerschmidt and A. P. McMahon, unpublished data).

Here we describe the molecular characterization of a spontaneous mouse mutation *Doublefoot* (*Dbf*) (Lyon et al., 1996), an autosomal dominant mutation mapping to a new gene locus on chromosome 1. *Dbf* mutation results in extreme polydactyly in all four limbs. Tibia and joint formation are also severely affected in the hindlimbs of both heterozygotes and homozygotes. In addition to these limb defects, the skull is abnormally broad and in homozygotes the maxillary processes fail to fuse. Moreover, the tail is often kinked. We present evidence that these *Dbf* phenotypes result from ectopic expression of *Ihh*, but that the *Dbf* mutation is genetically separable from *Ihh*, suggesting it has a long-range effect on *Ihh* regulation. Our results indicate that the two *Hh* family members, *Shh* and *Ihh*, which share overlapping expression in several regions of the mouse embryo, have similar polarizing activities. Our interpretation contrasts with that in a recent report by Hayes et al. (1998) which speculated that *Dbf* might encode a hitherto undiscovered activator of Smoothened (Smo), a seven-transmembrane protein thought to activate Hedgehog signaling.

MATERIALS AND METHODS

Mice

All animals were maintained under conventional conditions in the animal house of the MRC Mammalian Genetics Unit, Harwell. The *Dbf* mutant stock was maintained by crosses to 3H1 hybrids, which are (C3H/HeH × 101/H)F_1.

For molecular mapping, *Dbf*/+ females were crossed to *Mus spretus* males, and the F_1 female offspring backcrossed to C3H/HeH males. All offspring were typed with simple sequence length polymorphism (SSLP) markers.

To produce independent genetic linkage data, 3H1 females were crossed to *Mus spretus* males, and the F_1 female offspring backcrossed to C3H/HeH males.

To analyze the embryonic phenotypes of homozygous or heterozygous *Dbf* mutants, progeny embryos were obtained from the crosses of *Dbf*/+ × +/+ or *Dbf*/+ × *Dbf*/+. After 11.5 days, *Dbf* embryos were picked by the broad limb bud phenotypes. All 10.5 day embryos from the same litter were collected in the same tube.

SSLP markers

Genomic DNA was prepared from spleen and from tail biopsies using proteinase K-phenol/chloroform extraction. The polymerase chain reaction (PCR) was used to detect SSLPs. Primers *D1Mit22*, *D1Mit77*, *D1Mit24* and *D1Mit8* were purchased from Research Genetics (Huntsville, AL., USA). PCR was performed in a total volume of 10 μl containing 50 ng of genomic DNA, 6.6 μM forward and reverse primers, 100 mM tris-HCl (pH 8.4), 500 mM KCl, 1.5 mM $MgCl_2$, 200 μM dNTPs, 1 unit of Perkin-Elmer Cetus Taq polymerase. Amplifications were performed in a Perkin-Elmer-Cetus thermal cycler for 30 cycles of: 94°C for 60 seconds, 55°C for 90 seconds, 72°C for 90 seconds. Amplification products were separated by electrophoresis in 3% agarose gels.

Southern blot analysis

Ten micrograms of genomic DNA prepared from spleens were digested with the appropriate restriction endonuclease under standard conditions, separated by electrophoresis through 0.8% agarose gel at 2.5V/cm for 12-15 hours, and transferred onto Hybond-N+ membrane (Amersham, Life Sciences). The probes were labeled with [^{32}P]dCTP by nick translation, and hybridizations were performed at 64°C in a solution containing 10% dextran sulphate, 200 μg/ml herring sperm DNA, 1 mM EDTA, 6× SSC, 5× Denhardt's solution and 1% SDS. After hybridization, blots were washed with increasingly stringent washes ranging from 2× SSC, 20% SDS at 64°C to 0.1× SSC, 20% SDS prior to exposure to X-ray film for 1-3 days.

Gene markers

The *Ihh* locus was detected by a full length cDNA constructed by adding a *Nco*I/*Sac*I genomic fragment to the 5′-end of the partial *Ihh* cDNA clone reported previously (Echelard et al., 1993; Marigo et al., 1995). The 2.2 kb cDNA insert detected a major fragment of 8.5 kb in C3H DNA and a major fragment of 6.0 kb in *Mus spretus* DNA following digestion with *Bgl*II.

The *Pax3* probe, an approx. 1.2 kb *Eco*RI fragment of mouse cDNA, detected RFLV of 3 kb in C3H DNA and of 2.3 kb in *Mus spretus* DNA following digestion with *Taq*I (Goulding et al., 1991).

In situ hybridization and vibratome section

Whole-mount in situ hybridization using digoxigenin-labeled antisense RNA was performed as described by Wilkinson and Nieto (1993). The riboprobes used in this study have been described previously: *Shh* and *Ihh* (Echelard et al., 1993); *Fgf4* (Niswander and Martin, 1992); *Bmp2* (Lyons et al., 1989); *Ptc* (Goodrich et al., 1996) and *Hoxd13* (Dolle et al., 1991).

After whole-mount in situ hybridization, one of the limbs was cut off and embedded in 2% agarose (in PBS) at 50°C. The embedded sample was vibratome-sectioned at a thickness of 40 μm.

RESULTS

Limb skeleton abnormalities of *Dbf* mutants

The *Dbf* mutation is an autosomal dominant mutation which arose spontaneously. Homozygous *Dbf* mutants die in utero at around 14.5 days post coitum (d.p.c.). Typical heterozygous *Dbf* mutants have extreme preaxial polydactyly with 6 to 8 digits on all the four limbs (Fig. 1). In addition, the tibia and fibula are often shortened and bowed with gross twisting of ankles (Lyon et al., 1996). A similar phenotype has been observed in *Rim4*, *Hx* and *Xt* mutants, all of which exhibit preaxial polydactyly (Masuya et al., 1995). Digit duplication was clearly seen around 13.5 d.p.c. (Fig. 1A,B). However, digit 1, which has only two phalanges, is often missing, and there are two or more triphalangeal extra digits. In addition, fusion of digits, webbing of soft tissue and abnormal swelling of the ventral surface have been reported. Since the embryonic limb phenotypes of *Dbf*/*Dbf* and *Dbf*/+ are indistinguishable (Lyon et al., 1996), most of the *Dbf* mutants we studied here are heterozygous for the mutant allele.

Ihh is ectopically expressed in *Dbf* mutants

The duplicated digits in *Dbf* mutants suggest the existence of ectopic polarizing activity in the limb outside the endogenous ZPA. As *Shh* appears to encode the ZPA activity and ectopic *Shh* expression underlies preaxial polydactyly in several mutants, we examined *Shh* expression in *Dbf* mutants. At 11.5 d.p.c., *Dbf* mutant embryos exhibit a broadening of limb buds along the anterior-posterior axis. However, expression of *Shh* in the *Dbf* mutant is localized to the distal posterior margin in both the fore- and hindlimb in a pattern identical to that of wild-type embryos (Fig. 2A,B).

We next examined the molecular markers induced by polarizing activity such as *Fgf4*, *Bmp2* and *Hoxd13* in 11.5 d.p.c. wild-type and *Dbf* embryos (Fig. 3). In wild-type embryos, *Fgf4* expression is detected in the posterior AER and *Hoxd13* is expressed at a higher level in the distal posterior mesenchyme. In *Dbf* mutant embryos, ectopic *Fgf4* expression is detected in the anterior AER (Fig. 3B) and *Hoxd13* expression extends all the way to the anterior mesenchyme such that the expression domain is symmetric across the A-P axis (Fig. 3D). *Bmp2* exhibits a very dynamic expression pattern from 11 to 12.5 d.p.c. At 11 d.p.c. in the wild type, *Bmp2* expression is detected in the AER and the posterior and proximal limb margin (Fig. 4A,C) whereas in the *Dbf* mutant, *Bmp2* expression is detected in the distal part of the limb bud throughout the A-P axis in both fore-and hindlimbs (Fig. 4B,D). At 11.5 d.p.c., *Bmp2* is expressed in the future metacarpal region, interdigital area, the most distal mesenchyme and the AER in the forelimb of wild-type embryos (Fig. 4E). In the hindlimb, *Bmp2* expression is detected in the posterior-distal limb around the ZPA, as well as in the posterior-proximal limb margin and future metacarpal area (Fig. 4G). However, in the anterior forelimb of *Dbf* mutants, general and broad expression substituted for interdigital expression (Fig. 4F) and in the hindlimb, *Bmp2* expression extended all the way to the anterior limb bud (Fig. 4H). These data suggest that unlike all the other preaxial polydactyly mutants characterized to date, the *Dbf* mutation leads to ectopic polarizing activity outside the endogenous ZPA without altering the expression of *Shh*. Interestingly, in the metacarpel area at 11.5 d.p.c., the restricted and circular expression pattern of *Bmp2* extended posteriorly and anteriorly such that it looks like a thin band. At 12.5 d.p.c., *Bmp2* expression is detected exclusively in the interdigital region in the wild-type limb (Fig. 4I,K), but in the mutants, *Bmp2*

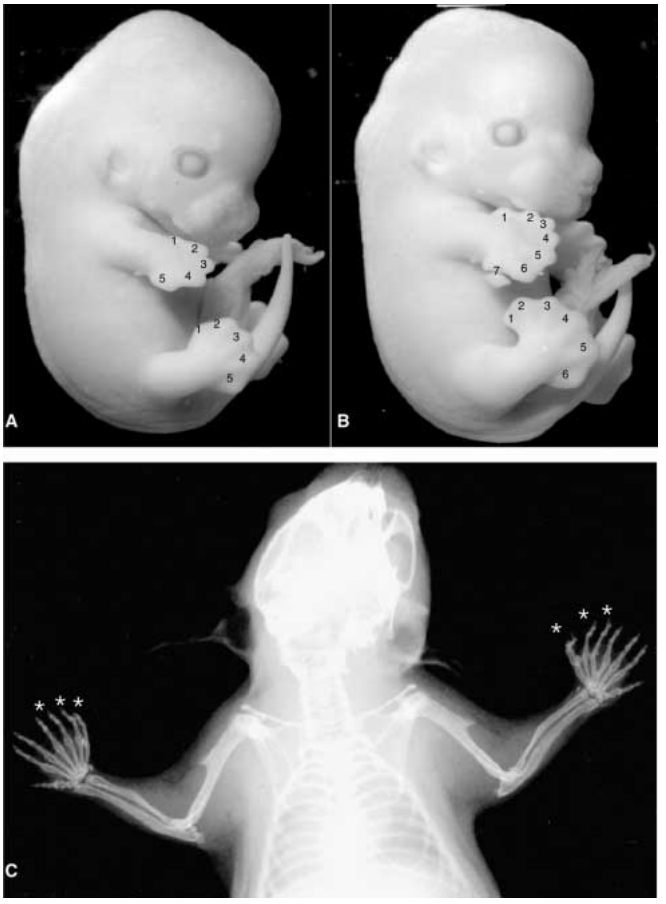

Fig. 1. Preaxial polydactyly in mice heterozygous for the *Dbf* mutation. At 13.5 d.p.c., each digit primordium can be clearly seen in both fore- and hindlimbs. (A) Wild-type embryos. The five digits in both fore- and hindlimb are numbered. (B) *Dbf* heterozygous mutant. There are 7 digits in the forelimb and 6 in the hindlimb. (C) X-ray photograph of the resulting forelimb skeleton of an adult *Dbf* heterozygous mutant. The anterior-most digit, digit 1 with two phalanges, is missing and there are three extra tri-phalangeal digits marked by *.

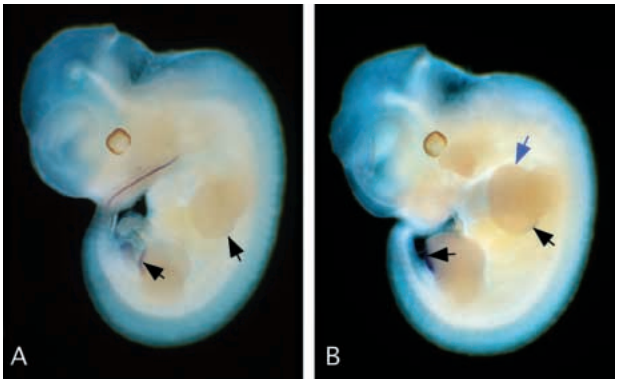

Fig. 2. *Shh* expression in embryos heterozygous for the *Dbf* mutation is not altered. *Shh* expression in 11.5 d.p.c. embryos was examined by whole-mount in situ hybridization. (A) Wild-type embryo. *Shh* is expressed in the distal posterior limb margin. (B) *Dbf* mutant embryo. *Shh* expression is unaltered. Note that the broadening of forelimb hand plate (indicated by a blue arrow) is already obvious at this stage. However, no *Shh* expression was detected outside the endogenous ZPA. Black arrows point to endogenous *Shh* expression.

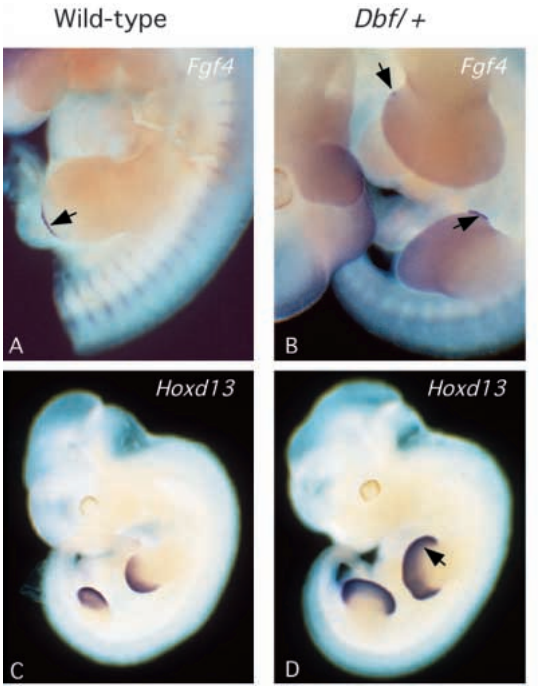

Fig. 3. Comparison of the expression patterns of *Fgf4* and *Hoxd13* in wild-type embryos and embryos heterozygous for the *Dbf* mutation. Whole-mount in situ hybridization was performed on 11.5 d.p.c. embryos. (A) Wild-type embryo. *Fgf4* expression is detected in the posterior AER (arrow). (B). *Dbf* mutant embryo. *Fgf4* was ectopically expressed in the anterior AER of both fore- and hindlimb buds (arrows). (C) Wild-type embryo. *Hoxd13* is expressed predominantly in the distal posterior limb. (D) *Dbf* mutant embryo. *Hoxd13* expression is equally strong in both the anterior (arrow) and posterior limb bud.

expression is missing in some interdigital areas (Fig. 4J,L) where ectopic digits will form.

Hedgehog signaling is associated with the transcriptional activation of *Ptc* which encodes a Hh receptor (Stone et al., 1996; for review see Tabin and McMahon, 1997). We examined the expression pattern of *Ptc* in *Dbf* mutants. At 11.5 d.p.c., *Ptc* expression extended all the way to the anterior limb margin (Fig. 5B) whereas in wild-type embryos it is localized to the posterior limb mesenchyme (Fig. 5A). In *Dbf* forelimbs, ectopic *Ptc* expression is stronger at the distal-anterior limb margin whereas in the hind limb, *Ptc* is more uniformly expressed across the distal A-P axis. *Ptc* is also ectopically expressed in the future femur region. These data suggest that ectopic activation of the *Hh* signaling pathway independent of *Shh* may be responsible for the observed phenotype. We also examined the expression pattern of transcriptional targets of Hedgehog signaling such as *Gli1* and *Gli2* and found that *Gli1* is similarly ectopically expressed as *Ptc* (Fig. 5D). However, *Gli2* was ectopically repressed in the distal most mesenchyme (Fig. 5H). Recently, a second mouse *Ptc* gene, *Ptc-2*, has been identified which shares overlapping expression pattern with *Ptc*, during several aspects of embryonic development (Motoyama et al., 1998). In the *Dbf* mutant, *Ptc-2* was similarly upregulated and ectopically activated (Fig. 5F) as *Ptc*, consistent with the view that *Ptc-2* may also be a transcriptional target of Hedgehog signaling during A-P patterning of the limb.

The *Dbf* mutation has been previously mapped to mouse chromosome 1, close to the *Ihh* locus. This prompted us to examine whether *Ihh* expression is affected by the *Dbf* mutation. Strong ectopic expression of *Ihh* is detected in the distal limb bud across the A-P axis of the *Dbf* mutant at 11.5 d.p.c. (Fig. 6B). As no ectopic *Ihh* expression is detected in *Dbf* mutants at 10.5 d.p.c. (data not shown), we infer that the onset of ectopic *Ihh* expression lies between 10.5 and 11.5 d.p.c. By 12.5 d.p.c., ectopic *Ihh* expression has decreased and becomes localized to the anterior limb bud (Fig. 6C). Strong ectopic *Ihh* expression can also be observed in the future femur region where *Ptc* and *Ptc-2* are also ectopically expressed (Fig. 7F,I). We also noticed that in both fore- and hindlimbs of *Dbf* mutants, *Ihh* is not ectopically expressed in the distal posterior limb margin where *Shh* is expressed (Fig. 6B). Examination of limb bud sections indicates that ectopic *Ihh* expression is restricted to the distal limb mesenchyme directly beneath the surface ectoderm (Fig. 6D,E). Taken together, these results suggest that ectopic expression of *Ihh* establishes an ectopic polarizing activity which perturbs the normal A-P limb patterning by the endogenous ZPA. As the distal mesenchyme is responsible for zeugopod and autopod development in the hindlimb after 10.5 d.p.c. (Milaire and Goffard, 1995), it seems likely that the abnormality of the tibia and fibula in *Dbf* mutants is also caused by ectopic *Ihh* expression. Ectopic *Ihh* expression is also detected in the metacarpal regions where expression of *Ptc* and *Bmp2* are also altered (Fig. 7D,E,G,H). This may cause the abnormally expanded and ventrally smooth handplate.

As joint abnormalities are seen in *Dbf* mutants, this raised the possibility that dorsal-ventral polarity may be reversed in certain regions of the limbs. To test this, whole-mount in situ hybridization was performed on 12.5 d.p.c. *Dbf* mutant embryos with *Lmx1b*, a dorsal determinant (Riddle et al., 1995; Cygan et al., 1997). *Lmx1b* expression is unaltered in *Dbf* mutant limbs when compared with wild-type embryos (data not shown), suggesting that the observed alteration along the D-V axis in *Dbf* mutants are independent of *Lmx1b*.

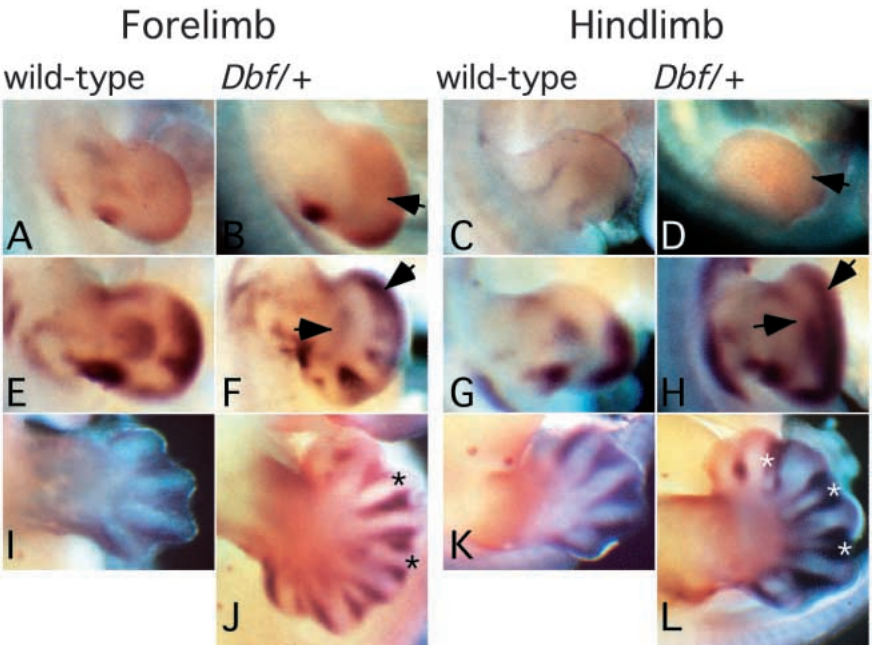

Fig. 4. Dynamic expression patterns of *Bmp2* in the developing limb buds are altered in *Dbf* heterozygous mutant mice. (A, E,I) *Bmp2* expression in the forelimbs of wild-type mice at 11,11.5 and 12.5 d.p.c. respectively. (B,F,J) *Bmp2* expression in the forelimbs of stage-matched *Dbf* heterozygous mutants. (C,G,K). *Bmp2* expression in the hindlimbs of wild-type mice at 11, 11.5 and 12.5 d.p.c. respectively. (D,H,L) *Bmp2* expression in the hindlimbs of stage matched *Dbf* mutants. In the *Dbf* heterozygous mutants, ectopic *Bmp2* expression is detected in a broad band across the AP axis at the distal part of both the forelimb (B) and hindlimb (D,H). At 11.5 d.p.c., digit primordia can be seen in the forelimbs and *Bmp2* expression starts to be detected in the interdigital area shown in E. At this stage, *Bmp2* can also be detected in the metacarpal region of both the fore- and hindlimbs. In the forelimb of same stage mutant (F), *Bmp2* expression can still be detected in a band-like domain in the anterior distal limb bud, where extra limb outgrowth is obvious and expression in the metacarpal region is narrowed and extends to both the anterior and posterior ends as a thin band. At 12.5 d.p.c., *Bmp2* expression is detected in the interdigital area of both the wild-type fore- and hind-limbs (I,K) whereas in the mutants, *Bmp2* expression is missing in some interdigital area shown by * (J, L). Arrows point to ectopic *Bmp2* expression.

Dbf mutants also have facial abnormalities and kinky tails suggesting that these phenotypes may also result from ectopic *Ihh* expression. We detected weak ectopic *Ihh* expression in the branchial arches and tail bud of *Dbf* mutant (Fig. 6B) at 11.5 d.p.c. At 12.5 d.p.c., *Dbf* mutants have broader facial processes and ectopic activation of *Ihh* was more obvious (Fig. 7E,F) accompanied by elevated expression of *Ptc*, *Ptc-2*, *Gli1* (Fig. 5B,D,F) and decreased expression of *Gli2* (Fig. 5H) in the branchial aches. However, no ectopic expression of *Ptc* was observed in the tail bud (Fig. 5B).

Molecular mapping of *Dbf* mutation

As a first attempt to determine the relationship between *Ihh* and the *Dbf* mutation, the *Dbf* mutation was further mapped using molecular markers. A total of 204 mice were typed with *D1Mit22*, *D1Mit24*, *D1Mit77* and *D1Mit8* microsatellite markers. The results indicate a complete co-segregation of *Dbf* with both *D1Mit77* and *D1Mit24*. Miller et al. (1996) found a 4.6 centimorgan (cM) interval between *D1Mit77* and *D1Mit24*. To check if the cosegregation we observed was due to an effect of the *Dbf* mutation, 79 mice from a (3H1 × *Mus spretus*)F_1 ×

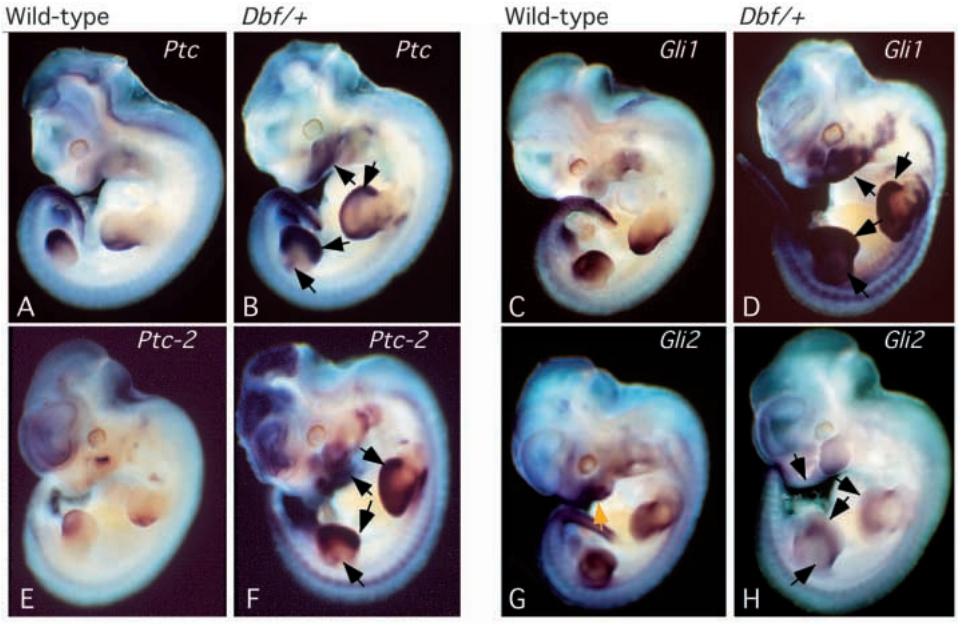

Fig. 5. *Hedgehog* targets are ectopically activated or repressed in the limb bud and branchial arches of embryos heterozygous for the *Dbf* mutation. Whole-mount in situ hybridization to 11.5 d.p.c. mouse embryos. (A,E,C,G) Wild-type embryos. (B,F,D,H) *Dbf* mutant embryos. *Ptc*, *Ptc-2*, *Gli-1* are ectopically activated and *Gli2* is ectopically repressed in the facial processes, the distal limb across the A-P axis and in the future femur region. Black arrows point to the ectopic activation (B,D,F) or repression (H). The yellow arrow in G points to the branchial arches where *Gli-2* is strongly expressed.

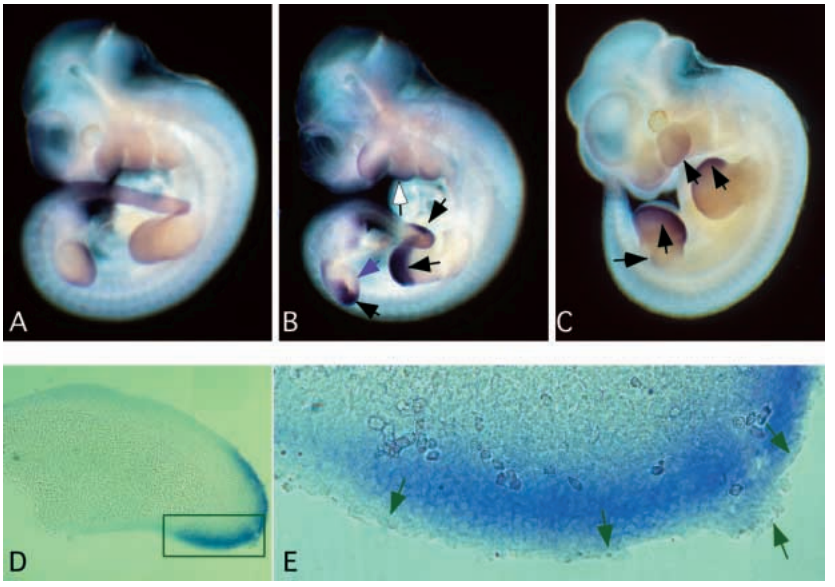

Fig. 6. *Ihh* is ectopically expressed in the distal limb, branchial arches and dorsal tail of embryos heterozygous for the *Dbf* mutation. Whole-mount in situ hybridization was performed at 11.5 and 12.5 d.p.c. (A) 11.5 d.p.c. wild-type embryo. No *Ihh* expression was detected in the limb bud. (B) 11.5 d.p.c. *Dbf* mutant embryo. *Ihh* expression was detected in the distal limb bud and tail bud. However, at the posterior margin where *Shh* was normally expressed, no *Ihh* expression was detected (purple arrow). Ectopic *Ihh* is also detected in the branchial arches (white arrow). (C) 12.5 d.p.c. *Dbf* mutant embryo. *Ihh* expression is down-regulated in the apical region whereas its expression in the anterior limb bud remained strong. Black arrows point to the ectopic *Ihh* expression pattern in the *Dbf* mutant (B,C). (D) Vibratome section of *Ihh* expression in the 11.5 d.p.c. limb bud of a *Dbf* mutant embryo. Ectopic *Ihh* expression in the distal limb bud was quite superficial and was absent in the 'core' mesenchyme. The boxed area in D is shown in higher magnification in E. (E) Ectopic *Ihh* expression was not detected in the distal ectoderm and AER (green arrows).

C3H/HeH backcross were typed with the four microsatellite markers. There were no crossovers between *D1Mit77* and *D1Mit24* indicating that the cosegregation of *D1Mit77* and *D1Mit24* is not an effect of the *Dbf* mutation.

An additional sample of 147 animals were typed for *D1Mit22* and *D1Mit8* and only recombinants between the two markers were subsequently typed for *D1Mit77* and *D12Mit24*. Of the 351 animals typed in total for *D1Mit22* and *D1Mit8*, 46 involved a crossover between the two markers (see Fig. 8. for haplotypes). These data give a distance of 13.1±1.8 cM between *D1Mit22* and *D1Mit8*. The number of recombination events between *D1Mit22* – (*D1Mit77*, *D1Mit24*, *Dbf*) – *D1Mit8* are respectively 26 and 20. The genetic distances (in centimorgans ± standard deviation) obtained are: *D1Mit22* – 7.4±1.4 – (*D1Mit77*, *D1Mit24*, *Dbf*) – 5.7±1.2 – *D1Mit8*. Of the 46 recombinant animals between *D1Mit22* and *D1Mit8*, 41 were successfully typed for *Ihh* and 39 for *Pax3*. Of the 41 typed for *Ihh*, 4 involved a crossover between *Dbf* and *Ihh*. Of the 39 typed for *Pax3*, 11 involved a crossover between *Dbf* and *Pax3*. In view of these results, both *Ihh* and *Pax3* can be excluded as candidate genes for the *Dbf* mutation. There are 19/41 recombination events between *D1Mit22* and *Ihh* and 6/39 between *Pax3* and *D1Mit8*.

The order of genes and SSLP markers was determined by minimizing the number of recombination events required to explain the allele distribution pattern. The mapping data indicate that *Ihh* maps between *D1Mit22* and *Dbf*, and *Pax3* maps between *Dbf* and *D1Mit8*. Based upon these data, the genetic distances (in centimorgans ± standard deviation) are: *D1Mit22* – 6.0±1.4 – *Ihh* – 1.3±0.7 – (*D1Mit77*, *D1Mit24*, *Dbf*) –3.7±1.2 – *Pax3* – 2.0±0.8 – *D1Mit8*. The genetic map is shown in Fig. 8. Together with the earlier results, these mapping data indicate that although the *Dbf* mutation leads to a dominant activation of *Ihh*, the *Dbf* mutation most likely lies several hundred kilobases away from the *Ihh* gene which is encoded by three exons spanning about 6 kilobases. If *Dbf* is a regulatory mutation, it may also affect the endogenous *Ihh* expression pattern. To test this, we examined *Ihh* expression in 12.5 d.p.c. wild-type, *Dbf*/+ and *Dbf/Dbf* embryos. These results indicate that *Ihh* is still expressed in its normal places in both *Dbf* heterozygotes and homozygotes (Fig. 7).

DISCUSSION

Polydactyly and *Ihh* expression

All of the previously characterized preaxial polydactyly mutants contain an ectopic anterior ZPA characterized by ectopic *Shh* expression. Here we show the first example of a polydactylous mutant, *Dbf*, which does not result from *Shh* expression. Rather, ectopic expression of another *Hedgehog* family member, *Ihh*, is detected in the distal limb mesenchyme. Thus, in agreement with studies in the chick (Vortkamp et al., 1996), *Ihh*, which is normally expressed later in limb development in association with cartilage development, is capable of altering limb polarity resulting in the formation of extra digits along the A-P axis, similar to those resulting from ectopic *Shh* activity.

All three *Hh* family members share a high degree of sequence similarity in the N-terminal region of the proteins. However, their comparative activities have not been rigorously addressed. For *Shh*, it has been shown in several assay systems that the signaling activity resides in the N-terminal part of the protein (Marti et al., 1995; Ericson et al., 1995; Roelink et al., 1995; Fan et al., 1995; Lopez-Martinez et al., 1995). In addition, all three mouse *Hhs*, like their *Drosophila* orthologue *Hh*, induce the expression of *Ptc* (Marigo et al., 1996; Marigo and Tabin, 1996; Goodrich et al., 1996; Bitgood and McMahon, 1995) which appears to encode the Shh and probably general Hh receptor (Stone et al., 1996; for review see Tabin and McMahon, 1997). Here we show that *Ptc-2* is ectopically expressed in the *Dbf* mutant in a similar fashion as *Ptc*. As ectopic presentation of Shh protein to later limb cultures is able to influence cartilage development in a manner similar to Ihh (Vortkamp et al., 1996), it seems very likely that at least for *Shh* and *Ihh*, their activities may be similar, if not equivalent. This result may have some significance as *Shh* and *Ihh* expression overlap at several sites in the developing

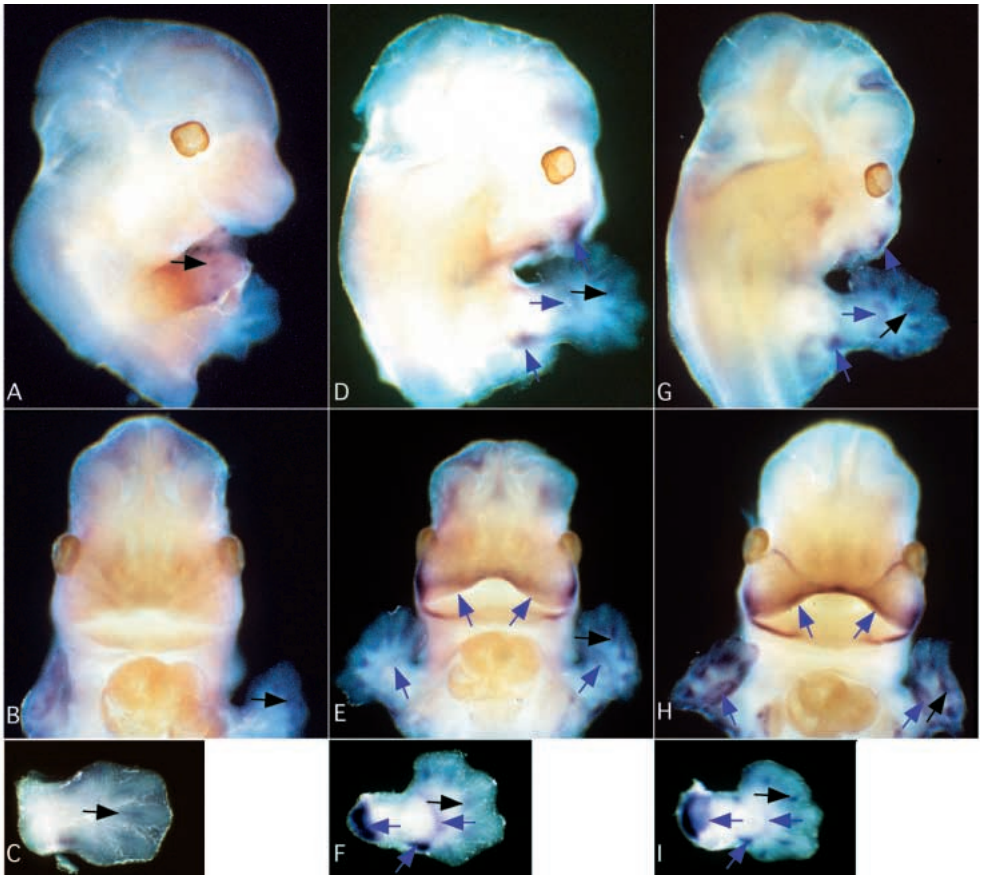

Fig. 7. Endogenous *Ihh* expression is not changed in both *Dbf* heterozygous and homozygous mutants. Whole-mount in situ hybridization was performed on embryos at 12.5 d.p.c. (A-C) Wild-type embryo; (A) lateral view, (B) ventral view, (C) hindlimb. At this stage, expression of *Ihh* in the hindlimb is very weak. (D-F) *Dbf* heterozygous embryo; (D) lateral view, (E) ventral view, (F) hindlimb. (G-I) *Dbf* homozygous embryo; (G) lateral view, (H) ventral view, (I) hindlimb. In both heterozygous and homozygous embryos, *Ihh* is still expressed in the cartilage as in wild-type embryos. Normal *Ihh* expression in the cartilage is indicated by black arrows. *Ihh* is also ectopically expressed in the branchial arches, dorsal and ventral metacarpal region and future elbow, indicated by purple arrows. The heterozygotes and homozygotes have broader and shorter facial processes as compared to wild-type embryos.

embryo, most notably in the gut endoderm (Bitgood and McMahon, 1995).

In *Dbf* mutants, the domain of ectopic *Ihh* expression is much broader and stronger than that of ectopic *Shh* expression at the anterior margin of other preaxial polydactyly mutants such as *lst* and *Xt* (Chan et al., 1995; Masuya et al., 1995). This difference most likely explains the difference between the *Dbf* phenotype and the phenotypes of all the other preaxial polydactyly mutations in the following aspects. (1) In *Dbf* mutants, there are generally more digits. It has been shown that a piece of ZPA tissue grafted to the anterior margin can lead to excessive growth of anterior mesenchyme in the chick limb (Cooke and Summerbell, 1981). It is thus likely that a broader polarizing activity due to the broader *Ihh* expression causes more extensive growth in the distal mesenchyme, eventually leading to the formation of larger number of supernumerary digits. (2) Compared to ectopic *Shh* expression in other preaxial polydactyly mutants such as *Xt* and *Hx* (Buscher and Ruther, 1998), ectopic *Ihh* expression in the *Dbf* mutant is broader and stronger. This may explain why *Gli2* is ectopically repressed in the distal limb region whereas no change in *Gli2* expression was observed in either *Xt* or *Hx* mutants (Buscher and Ruther, 1998). This is also consistent with the expression of *Gli2* in normal limb which is absent from the *Shh*-expressing ZPA. Moreover, $Gli2^{-/-};Gli3^{-/+}$ compound mutants have a more profound preaxial polydactyly when compared to $Gli3^{+/-}$ (Mo et al., 1997) embryos, indicating that *Gli2* and *Gli3* may share similar functions in Hedgehog signaling in the limb. (3) All of the digits in *Dbf* heterozygotes are arranged in a single group which is symmetric along the A-P axis. In contrast, in the heterozygotes of other preaxial polydactyly mutants the duplicated digits are often located anterior to the endogenous digit 1. *Ihh* ectopic expression appears to be uniform along the A-P axis at 11.5 d.p.c. except in the region of the endogenous ZPA where *Shh* itself is expressed. As recent evidence indicates that the concentration of Shh is the primary determinant of digit identity (Yang et al., 1997), approximately equivalent expression of similar polarizing activity across the A-P axis would predict the generation of digits with similar pattern. However, at 12-12.5 d.p.c., *Ihh* ectopic expression is stronger at the anterior margin. Therefore, the endogenous and ectopic polarizing activity appears to affect the posterior and anterior margin more than the apical limb tip. This conclusion is consistent with the observed pattern of digit duplication in

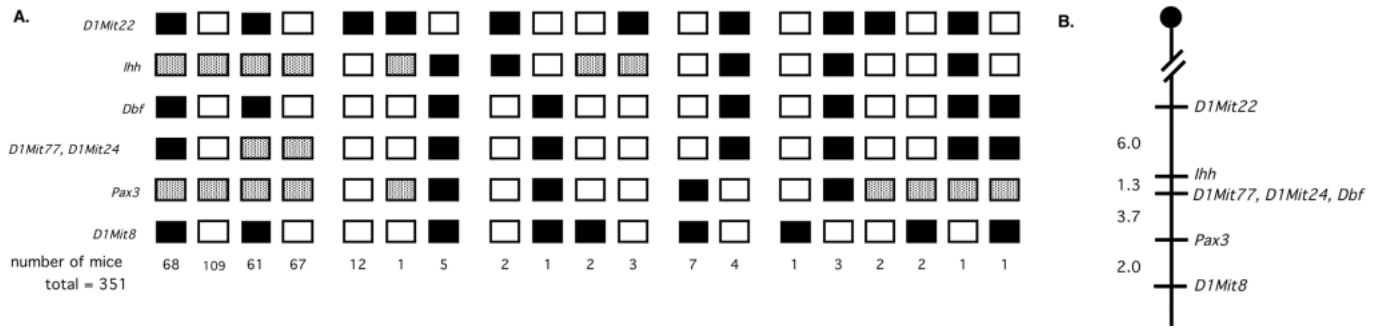

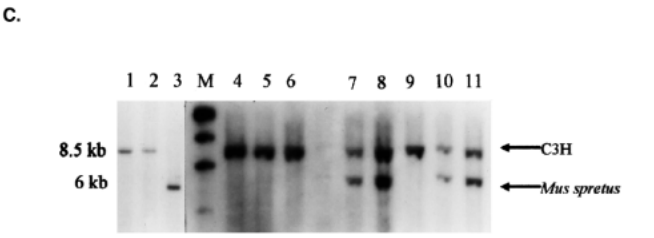

Fig. 8. Mapping *Dbf* mutation relative to *Ihh* on mouse chromosome one. (A) Haplotype analysis of a total of 351 mice. The loci that have been typed are shown on the left. The numbers of each haplotype are listed below. Open boxes represent a *Mus spretus* allele and black boxes represent a laboratory mouse allele. Missing data are represented by stippled boxes. These data include those of Lyon et al. (1996). (B) Genetic map of mouse chromosome 1. Genetic distances in cM are on the left. (C) Southern blot analysis of *Ihh* in controls and offspring from the interspecific backcross. Lanes 1, 2 and 3 are DNA prepared respectively from C3H, 101 and *Mus spretus*; M, *Hin*dIII marker; lane 4 to 11, DNA prepared from the interspecific backcross offspring.

which the most anterior digit appears to adopt a posterior fate (Digit 5 fate). The other additional anterior digits all appear similar in morphology. (4) The development of hindlimb zeugopod and ankle joint is more severely affected. Both the tibia (anterior bone) and the fibula (posterior bone) are shortened and bent. Ectopic *Ihh* expression in the hindlimb bud of the *Dbf* mutant embryo extends more posteriorly and proximally than that of ectopic *Shh* in other preaxial polydactyly mutants, consequently, the fibula is also affected in the *Dbf* mutant.

Alterations in D-V polarity are associated with abnormal joint formation, but we observed no change in the expression of *Lmx1b*, a dorsal determinant (Riddle et al., 1995; Cygan et al., 1997) in *Dbf* mutants. Based on this observation, it is most likely that the joint abnormality in *Dbf* mutants is due to unbalanced A-P growth, such that the feet are twisted along the D-V axis. However, we can not rule out the possibility that expression of an unknown gene downstream of *Lmx1b*, which also serves to pattern the D-V axis, is altered in *Dbf* mutants.

Broad ectopic expression of *Ihh* in the distal mesenchyme and tail bud may also be the cause of other aspects of the phenotype such as swollen and smooth ventral limb surface and kinky tails. Indeed, we observed ectopic *Ihh* expression in the metacarpal region of all four limbs in *Dbf* mutants. One possible explanation is that the normal balance between growth and patterning is disrupted in the presence of ectopic *Ihh*. It has been shown that Bmp signaling in the interdigital area may regulate interdigital cell death (Zou and Niswander, 1996; Ganan et al., 1996; Yokouchi et al., 1996). Since in *Dbf* mutants *Bmp2* expression in the distal anterior mesenchyme is changed and the interdigital expression disappeared in some areas, it is possible that this leads to the soft tissue webbing of the anterior digits or the formation of extra digits. In all of the *Dbf* mutant embryos we have analyzed, none displayed ectopic *Ihh* expression in the brain. Thus, the reported brain phenotype (Lyon et al., 1996) may be unrelated to the mis-regulation of *Ihh* or may result from ectopic expression at a different stage of development. Analysis of *Dbf* and *Ihh* double mutants will be required to further demonstrate that the phenotypes of *Dbf* mutants are solely due to *Ihh* ectopic expression.

Our genetic mapping data localized *Dbf* to a region approximately 1.3 cM away from the *Ihh* locus. In the mouse, this genetic distance corresponds to a physical distance of approximately 2600 kb (Lyon et al., 1996). The observation that ectopic *Ihh* expression is responsible for extra digit formation in *Dbf* mutants further suggests that the mutation is unlikely to be contained within the coding region of *Ihh* and we were unable to detect any restriction fragment length polymorphism after analyzing about 8 kb 5′ and 8 kb 3′ of the *Ihh* gene (data not shown). Thus it is not clear how the *Dbf* mutation causes ectopic expression of *Ihh*. Several possible models could explain the results. For example, *Dbf* may contain a DNA rearrangement which acts in *cis* to place *Ihh* transcription under the control of an enhancer element in a neighboring gene normally expressed in the distal limb, facial processes and tail. A precedent exists in which mutations affect gene expression over a long range. For example, it has been shown that two mutant alleles of *steel* (*Sl*), *Steel-panda* (Sl^{pan}) and *Steel-contrasted* (Sl^{con}), contain DNA rearrangements located 100-200 kb upstream of the coding sequences (Bedell et al., 1995). Such a rearrangement would be consistent with the dominant phenotype. Alternatively, a *cis*-acting rearrangement may lead to the disruption of a negative regulatory region controlling *Ihh* expression. *Dbf* may also act in *trans* by inactivating a transcription factor which normally inhibits the expression of *Ihh* in the distal limb. Given the dominant phenotype, repression at the *Ihh* locus would have to be dose-sensitive in this model. Alternatively, ectopic expression of a transcription factor which directs the activation of *Ihh* could explain the results. Further mapping and characterization of *Dbf* will be required to distinguish between these possibilities. However, in view of the large genetic distances involved, and the strong likelihood that *Dbf* may result in a regulatory mutation, this may be a difficult task.

Interestingly, as the endogenous *Ihh* expression pattern does not seem to be affected by the *Dbf* mutation, it is likely that *Dbf* results in ectopic *Ihh* expression while leaving normal *Ihh* regulation intact.

In conclusion, our data suggest that the biological mediator of the *Dbf* limb phenotype (and probably the face as well) is ectopic Ihh signaling which at this stage mimics the polarizing activity of Shh. Whilst our study was under review, Hayes et al. (1998) published a study on *Dbf* mutants. Although both studies agree substantially on most of the data, they differ in the key data, which is, *Ihh* ectopic expression and interpretation. Hayes et al. invoked a novel (as yet unidentified) ligand for Smoothened to account for the ectopic polarizing activity, failing to address the possibility of another Hedgehog member's involvement. In our view, ectopic Ihh activity simply explains both sets of data, including the non-cell autonomy of ectopic polarizing activity reported by Hayes et al. (1998).

We thank Benoit St-Jacques for molecular mapping of the *Ihh* locus, Karen Steel for providing the *Pax3* probe and Sue Morse for animal care. We also thank Pao-Tien Chuang and Jenny Cygan for critical reading of the manuscript. Yingzi Yang is supported by a postdoctoral fellowship from the Cancer Research Fund of the Damon Runyon-Walter Winchell Foundation. This research is supported by EU contract no. CHRX-CT93-0181 and work in A. P. McMahon's laboratory is supported by an NIH grant NS33642.

REFERENCES

Bedell, M. A., Brannan, C. I., Evans, E. P., Copela, N. G., Jenkins, N. A. and Donovan, P.J. (1995). DNA rearrangements located over 100 kb 5′ of the Steel (Sl)-coding region in Steel-panda and Steel-contrasted mice deregulate Sl expression and cause female sterility by disrupting ovarian follicle development. *Genes Dev.* **9**, 455-470.

Bitgood, M. J. and McMahon, A. P. (1995). Hedgehog and Bmp genes are coexpressed at many diverse sites of cell-cell interaction in the mouse embryo. *Dev. Biol.* **172**, 126-138.

Buscher, D., Bosse, B., Heymer, J. and Ruther, U. (1997). Evidence for genetic control of Sonic hedgehog by Gli3 in mouse limb development. *Mech. Dev.* **62**, 175-182.

Buscher, D. and Ruther, U. (1998). Expression profile of Gli family members and Shh in normal and mutant mouse limb development. *Dev. Dyn.* **211**, 88-96.

Chan, D. C., Laufer, E., Tabin, C. and Leder, P. (1995). Polydactylous limbs in Strong's Luxoid mice result from ectopic polarizing activity. *Development* **121**, 1971-1978.

Charite, J., de Graaff, W., Shen, S. and Deschamps, J. (1994). Ectopic expression of Hoxb-8 causes duplication of the ZPA in the forelimb and homeotic transformation of axial structures. *Cell* **78**, 589-601.

Cooke, J. and Summerbell, D. (1981). Control of growth related to pattern specification in chick wing-bud mesenchyme. *J. Embryol. Exp. Morphol.* **65, Supplement**, 169-185.

Crossley, P. and Martin, G. (1995). The mouse Fgf8 gene encodes a family of polypeptides and is expressed in regions that direct outgrowth and patterning in the developing embryo. *Development* **121**, 439-451.

Cygan, J., Johnson, R. and McMahon, A. (1997). Novel regulatory interactions revealed by studies of murine limb pattern in Wnt-7a and En-1 mutants. *Development* **124**, 5021-5032.

Dolle, P., Izpisua-Belmonte, J. C., Boncinelli, E. and Duboule, D. (1991). The Hox-4.8 gene is localized at the 5′ extremity of the Hox-4 complex and is expressed in the most posterior parts of the body during development. *Mech, Dev.* **36**, 3-13.

Dominguez, M., Brunner, M., Hafen, E. and Basler, K. (1996). Sending and receiving the hedgehog signal: control by the Drosophila Gli protein Cubitus interruptus. *Science* **272**, 1621-1625.

Echelard, Y., Epstein, D. J., St-Jacques, B., Shen, L., Mohler, J., McMahon, J. A. and McMahon, A. P. (1993). Sonic hedgehog, a member of a family of putative signaling molecules, is implicated in the regulation of CNS polarity. *Cell* **75**, 1417-1430.

Ericson, J., Muhr, J., Placzek, M., Lints, T., Jessell, T. M. and Edlund, T. (1995). Sonic hedgehog induces the differentiation of ventral forebrain neurons: a common signal for ventral patterning within the neural tube. *Cell* **81**, 747-756.

Fallon, J. F, Lopez, A., Ros, M. A., Savage, M. P., Olwin, B. B. and Simandl, B. K. (1994). FGF-2: apical ectodermal ridge growth signal for chick limb development. *Science* **264**, 104-107.

Fan, C. M., Porter, J. A., Chiang, C., Chang, D. T., Beachy, P. A. and Tessier-Lavigne, M. (1995). Long-range sclerotome induction by sonic hedgehog: direct role of the amino-terminal cleavage product and modulation by the cyclic AMP signaling pathway. *Cell* **81**, 457-465.

Ganan, Y., Macias, D., Duterque-Coquillaud, M., Ros, M. A. and Hurle, J. M. (1996). Role of TGF beta s and BMPs as signals controlling the position of the digits and the areas of interdigital cell death in the developing chick limb autopod. *Development* **122**, 2349-2357.

Goodrich, L. V., Johnson, R. L., Milenkovic, L., McMahon, J. A. and Scott, M. P. (1996). Conservation of the hedgehog/patched signaling pathway from flies to mice: induction of a mouse patched gene by Hedgehog. *Genes Dev.* **10**, 301-312.

Goulding, M. D., Chalepakis, G., Deutsch, U., Erselius, J. R. and Gruss, P. (1991). Pax-3, a novel murine DNA binding protein expressed during early neurogenesis. *EMBO J.* **10**, 1135-1147.

Hayes, C., Brown, J. M., Lyon, M. F. and Morriss-Kay, G. M. (1998). Sonic hedgehog is not required for polarizing activity in the Doublefoot mutant mouse limb bud. *Development* **125**, 351-357.

Hui, C. C. and Joyner, A. L. (1993). A mouse model of greig cephalopolysyndactyly syndrome: the extra-toes mutation contains an intragenic deletion of the Gli3 gene. *Nat. Genet.* **3**, 241-246.

Johnson, R. L. and Tabin, C. J.(1997). Molecular models for vertebrate limb development. *Cell* **90**, 979-990.

Laufer, E., Nelson, C. E., Johnson, R. L., Morgan, B. A. and Tabin, C. (1994). Sonic hedgehog and Fgf-4 act through a signaling cascade and feedback loop to integrate growth and patterning of the developing limb bud. *Cell* **79**, 993-1003.

Loomis, C., Kimmel, R., Tong. C. X., Michaud, J. and Joyner, A. (1998). Analysis of the genetic pathway leading to formation of ectopic apical ectodermal ridges in mouse Engrailed-1 mutant limbs. *Development* **125**, 1137-1148.

Lopez-Martinez, A., Chang, D. T., Chiang, C., Porter, J. A., Ros, M. A., Simandl, B. K., Beachy, P. A. and Fallon, J. F. (1995). Limb-patterning activity and restricted posterior localization of the amino-terminal product of Sonic hedgehog cleavage. *Curr. Biol.* **5**, 791-796.

Lyon, M. F., Quinney, R., Glenister, P. H., Kerscher, S., Guillot, P. and Boyd, Y. (1996). Doublefoot: a new mouse mutant affecting development of limbs and head. *Genet. Res.* **68**, 221-231.

Lyon, M. F., Rastan, S. and Brown, S. D. M., (1996). *Genetic Variants and Strains of the Laboratory Mouse*. Oxford University Press.

Lyons, K. M., Pelton, R. W. and Hogan, B. L. (1989). Patterns of expression of murine Vgr-1 and BMP-2a RNA suggest that transforming growth factor-beta-like genes coordinately regulate aspects of embryonic development. *Genes Dev.* **3**, 1657-1668.

Marigo, V., Roberts, D. J., Lee, S. M., Tsukurov, O., Levi, T., Gastier, J. M., Epstein, D. J., Gilbert, D. J., Copeland, N. G. and Seidman, C. E. (1995). Cloning, expression, and chromosomal location of SHH and IHH: two human homologues of the Drosophila segment polarity gene hedgehog. *Genomics* **28**, 44-51.

Marigo, V., Scott, M. P., Johnson, R. L., Goodrich, L. V. and Tabin, C. J. (1996). Conservation in hedgehog signaling: induction of a chicken patched homolog by Sonic hedgehog in the developing limb. *Development* **122**, 1225-1233.

Marigo, V. and Tabin, C. J. (1996). Regulation of patched by sonic hedgehog in the developing neural tube. *Proc. Natl. Acad. Sci. USA* **93**, 9346-9351.

Marti, E., Bumcrot, D. A., Takada, R. and McMahon, A. P. (1995). Requirement of 19K form of Sonic hedgehog for induction of distinct ventral cell types in CNS explants. *Nature* **375**, 322-325.

Masuya, H., Sagai, T., Moriwaki, K. and Shiroishi, T. (1997). Multigenic control of the localization of the zone of polarizing activity in limb morphogenesis in the mouse. *Dev. Biol.* **182**, 42-51.

Masuya, H., Sagai, T., Wakana, S., Moriwaki, K. and Shiroishi, T. (1995). A duplicated zone of polarizing activity in polydactylous mouse mutants. *Genes Dev.* **9**, 1645-1653.

Milaire, J. and Goffard, J. C. (1995). Histological analysis of limb defects

induced in developing limb buds of NMRI mouse embryos after oral administration of 3-3-dimethyl-1-phenyltriazene (DMPT) to their mother on day 10 of gestation. *Eur. J. Morphol.* **33**, 491-508.

Miller, J. C., et al. (1996). SSLP/Microsatellite genetic linkage map of the mouse. In *Genetic Variants and Strains of the Laboratory Mouse*, 3rd edn (ed. Lyon M. F., Rastan S., and Brown S. D. M.), pp. 1671-1755. Oxford: Oxford University Press.

Mo, R., Freer, A. M., Zinyk, D. L., Crackower, M. A., Michaud, J., Heng, H. H., Chik, K. W., Shi, X. M., Tsui, L. C., Cheng, S. H., Joyner, A. L. and Hui, C. (1997). Specific and redundant functions of Gli2 and Gli3 zinc finger genes in skeletal patterning and development. *Development* **124**,113-123.

Motoyama, J., Takabatake, T., Takeshima, K. and Hui, C. (1998). Ptch2, a second mouse Patched gene is co-expressed with Sonic hedgehog. *Nat. Genet.* **18**,104-106.

Niswander, L. and Martin, G. R. (1992). Fgf-4 expression during gastrulation, myogenesis, limb and tooth development in the mouse. *Development* **114**, 755-768.

Niswander, L., Jeffrey, S., Martin, G. R. and Tickle, C. (1994). A positive feedback loop coordinates growth and patterning in the vertebrate limb. *Nature* **371**, 609-612.

Niswander, L., Tickle, C., Vogel, A., Booth, I. and Martin, G. R. (1993). FGF-4 replaces the apical ectodermal ridge and directs outgrowth and patterning of the limb. *Cell* **75**, 579-587.

Parr, B. A. and McMahon, A. P. (1995). Dorsalizing signal Wnt-7a required for normal polarity of D-V and A-P axes of mouse limb. *Nature* **374**, 350-353.

Qu, S., Niswender, K. D., Ji, Q., van der Meer, R., Keeney, D., Magnuson, M. A. and Wisdom, R. (1997). Polydactyly and ectopic ZPA formation in Alx-4 mutant mice. *Development* **124**, 3999-4008.

Riddle, R. D., Ensini, M., Nelson, C., Tsuchida, T., Jessell, T. M. and Tabin, C. (1995). Induction of the LIM homeobox gene Lmx1 by WNT7a establishes dorsoventral pattern in the vertebrate limb. *Cell* **83**, 631-640.

Riddle, R. D., Johnson, R. L., Laufer, E. and Tabin, C. (1993). Sonic hedgehog mediates the polarizing activity of the ZPA. *Cell* **75**, 1401-1416.

Roelink, H., Porter, J. A., Chiang, C., Tanabe, Y., Chang, D. T., Beachy, P. A. and Jessell, T. M. (1995). Floor plate and motor neuron induction by different concentrations of the amino-terminal cleavage product of sonic hedgehog autoproteolysis. *Cell* **81**, 445-455.

Stone, D. M., Hynes, M., Armanini, M., Swanson, T. A., Gu, Q., Johnson, R. L., Scott, M. P., Pennica, D., Goddard, A., Phillips, H., Noll, M., Hooper, J. E., de Sauvage, F. and Rosenthal, A. (1996). The tumour-suppressor gene patched encodes a candidate receptor for Sonic hedgehog. *Nature* **384**, 129-134.

Tabin, C. J. and McMahon, A. P. (1997). Recent advances in Hedgehog signaling. *Trends Cell Biol.* **7**, 442-446.

Vortkamp, A., Franz, T., Gessler, M. and Grzeschik, K. H. (1992). Deletion of GLI3 supports the homology of the human Greig cephalopolysyndactyly syndrome (GCPS) and the mouse mutant extra toes (Xt). *Mamm. Genome* **3**, 461-463.

Vortkamp, A., Lee, K., Lanske, B., Segre, G. V., Kronenberg, H. M. and Tabin, C. J. (1996). Regulation of rate of cartilage differentiation by Indian hedgehog and PTH-related protein. *Science* **273**, 613-622.

Wilkinson, D. G. and Nieto, M. A. (1993). Detection of messenger RNA by in situ hybridization to tissue sections and whole mounts. *Methods Enzymol.* **225**, 361-373

Yang, Y., Drossopoulou, G., Chuang, P. T., Duprez, D., Marti, E., Bumcrot, D., Vargesson, N., Clarke, J., Niswander, L., McMahon, A. and Tickle, C. (1997). Relationship between dose, distance and time in Sonic Hedgehog-mediated regulation of anteroposterior polarity in the chick limb. *Development* **124**, 4393-4404.

Yokouchi, Y., Sakiyama, J., Kameda, T., Iba, H., Suzuki,A., Ueno, N. and Kuroiwa, A. (1996). BMP-2/-4 mediate programmed cell death in chicken limb buds. *Development* **122**, 3725-3734.

Zou, H. and Niswander, L. (1996). Requirement for BMP signaling in interdigital apoptosis and scale formation. *Science* **272**, 738-741. *Science* **272**, 738-741.